View metadata, citation and similar papers at core.ac.uk

brought to you by CORE

provided by Elsevier - Publisher Connector

Biochimica et Biophysica Acta 1798 (2010) 1934–1943

Contents lists available at ScienceDirect

Biochimica et Biophysica Acta

journal homepage: www.elsevier.com/locate/bbamem

Structural contributions to the intracellular targeting strategies of antimicrobial peptides

Yun Lan, Yan Ye, Justyna Kozlowska, Jenny K.W. Lam, Alex F. Drake, A. James Mason *

King's College London, Pharmaceutical Science Division, 150 Stamford Street, London, SE1 9NH, UK

ARTICLE INFO

Article history:
Received 22 March 2010
Received in revised form 2 July 2010
Accepted 6 July 2010
Available online 15 July 2010

Keywords:
Peptide antibiotics
CD spectroscopy
buforin II
magainin 2
pleurocidin
DNA binding

ABSTRACT

The interactions of cationic amphipathic antimicrobial peptides (AMPs) with anionic biological membranes have been the focus of much research aimed at improving the activity of such compounds in the search for therapeutic leads. However, many of these peptides are thought to have other polyanions, such as DNA or RNA, as their ultimate target. Here a combination of fluorescence and circular dichroism (CD) spectroscopies has been used to assess the structural properties of amidated versions of buforin II, pleurocidin and magainin 2 that support their varying abilities to translocate through bacterial membranes and bind to double stranded DNA. Unlike magainin 2 amide, a prototypical membrane disruptive AMP, buforin II amide adopts a poorly helical structure in membranes closely mimicking the composition of Gram negative bacteria, such as *Escherichia coli*, and binds to a short duplex DNA sequence with high affinity, ultimately forming peptide–DNA condensates. The binding affinities of the peptides to duplex DNA are shown to be related to the structural changes that they induce. Furthermore, CD also reveals the conformation of the bound peptide buforin II amide. In contrast with a synthetic peptide, designed to adopt a perfect amphipathic α-helix, buforin II amide adopts an extended or polyproline II conformation when bound to DNA. These results show that an α-helix structure is not required for the DNA binding and condensation activity of buforin II amide.

© 2010 Elsevier B.V. All rights reserved.

1. Introduction

The wide spectrum and rapid bactericidal activity of antimicrobial peptides has made them the focus of much research, aiming to add to the current arsenal of antibiotics whose effectiveness is being severely eroded by the increased prevalence of bacteria resistant to one or more classical antibiotics [1–4]. Considerable focus has been placed on the membrane disruptive properties of cationic amphipathic peptides, although it is recognized that many peptides may have alternative bactericidal mechanisms requiring them to penetrate bacteria and interfere with metabolic processes [5,6]. One such peptide, buforin II derived from the Asian toad *Bufo gargarizans*, has been shown to penetrate bacteria, inhibiting cellular functions [7]. Considering the demonstrated therapeutic efficacy of buforin II in a rat model of *Acinetobacter baumannii* sepsis [8], understanding the bactericidal strategy of buforin II and the underpinning structural contributions will offer a new avenue in the pursuit of therapeutically relevant peptide based antibiotics. In comparison with magainin 2, a cationic amphipathic peptide with well characterized membrane disruptive properties, buforin II binds DNA and RNA from *Escherichia coli* with a much greater affinity [7]. However, the nature of the peptide-nucleic acid interactions and the mechanisms that promote peptide binding are poorly understood.

To gain an improved understanding of these processes, we have used a combined circular dichroism (CD) and fluorescence approach to characterize the binding of buforin II and C-terminal amidated versions of buforin II, pleurocidin, magainin 2 and two tryptophan containing analogues (buforin F10W, magainin F5W) to mixed anionic lipid membranes as well as a short 15 base pair stretch of duplex DNA which is identical to that used in a recent molecular dynamics simulation study [9]. Cationic AMPs are often amidated at the C-terminus to increase activity and in the present study we have studied amidated versions of buforin II and magainin 2, comparing like with like, but have also examined the binding of the non-amidated form of buforin II to assess the contribution of this modification. In contrast with magainin 2 amide and pleurocidin amide, buforin II amide does not adopt significant α-helix conformation in model membranes mimicking those of Gram negative bacteria. Buforin II amide was observed to bind to DNA more readily than magainin 2 amide, as expected, and ψ condensates were indicated by the presence of circular intensity differential light scattering (CIDS). A sigmoidal response was observed in thiazole orange fluorescence intercalator displacement (FID) assays for buforin II amide but not for magainin 2 amide unless the phenylalanine at position 5 in magainin 2 amide was substituted by tryptophan (magainin F5W amide). Finally, the conformation of buforin II amide bound to DNA was shown to be

* Corresponding author. Tel.: +44 207 848 4813; fax: +44 207 848 4800.
E-mail address: james.mason@kcl.ac.uk (A.J. Mason).

0005-2736/$ – see front matter © 2010 Elsevier B.V. All rights reserved.
doi:10.1016/j.bbamem.2010.07.003

extended (probably P_{II}), not α-helical as suggested by the molecular dynamics simulation study [9]. The fundamentally different structural properties of buforin II amide, pleurocidin amide and magainin 2 amide can therefore be understood to be crucial in underpinning their distinct antibacterial strategies.

2. Materials and methods

2.1. Peptides, lipids, DNA and E. coli

Peptides (Table 1) were purchased from either EZBiolab (Carmel, IN) or Pepceuticals Ltd (Nottingham, UK) as desalted grade. Further HPLC purification was performed using methanol/water gradients. The lipids 1-palmitoyl-2-oleoyl-*sn*-glycero-3-phosphatidylcholine (POPC), 1-palmitoyl-2-oleoyl-*sn*-glycero-3-phosphatidylglycerol (POPG), 1-palmitoyl-2-oleoyl-*sn*-glycero-3-phosphatidylethanolamine (POPE), dimyristoyl-*sn*-glycero-3-phosphatidylcholine (DMPC) and dimyristoyl-*sn*-glycero-3-phosphatidylglycerol (DMPG) were obtained from Avanti Polar Lipids, Inc. (Alabaster, AL) and used without further purification. DNA duplex, as described previously [9], (AAA TAC ACT TTT GGT and complement, Mw duplex 9141.1, $\varepsilon = 233{,}145.9\ \text{L mole}^{-1}\ \text{cm}^{-1}$) was from Integrated DNA Technologies (Coralville, IA). *E. coli* (NCTC 9001) and *E. coli* TOP10 were gifts from K.D Bruce (King's College London) and C. Junkes (FMP, Berlin), respectively. All other reagents were analytical grade or better.

2.2. Liposome preparation

Samples with different lipid compositions were prepared (molar ratios in brackets): DMPC/DMPG (80:20), POPC/POPG (80:20) and POPE/POPG (80:20). For the binary lipid mixtures a total of around 7 mg lipids per sample were dissolved and mixed in chloroform and dried under rotor-evaporation at room temperature. In order to remove all organic solvent, the lipid films were exposed to vacuum overnight. The films were then rehydrated with 2 ml of 5 mM Tris-amine buffer at pH 7.0 at room temperature. Samples were then extruded, passaged eleven times through a 100-nm filter at room temperature. Extrusion rendered the liposomes optically transparent while the liposome sizes, measured on a Zetaplus (Brookhaven Instruments Corp., Long Island, NY), were typically in the region of 127 nm (DMPC/DMPG), 100 nm (POPC/POPG) and 128 nm (POPE/POPG) with polydispersity between 0.08 and 0.1.

2.3. Circular dichroism

Spectra were acquired on a Chirascan spectrometer (Applied Photophysics, Leatherhead, UK). Liposome samples were maintained at 37 °C while DNA binding experiments were performed at room temperature. For liposome experiments, spectra were recorded from 260 to 185 nm for liposomes composed of lipids with saturated acyl chains or from 260 to 195 nm when monounsaturated acyl chains were present. Lipid suspension was added to a 0.5-mm cuvette at a final concentration of 4.8 mM and then a few μl of a concentrated peptide solution were added and thoroughly mixed to give a final peptide concentration of 24 μM and a peptide-to-lipid molar ratio of 1:200. In processing, a spectrum of the peptide free suspension or solution was subtracted and Savitsky–Golay smoothing with a convolution width of 5 points applied. Secondary structure analyses were performed using CDPro [10]. For DNA measurements both near and far-UV CD spectra were obtained. Near-UV measurements were performed in a 10 mm cell, recording from 340 to 220 nm; far-UV measurements were performed on the same sample in 1 mm cells recording from 260 to 185 nm. DNA was prepared at a concentration of 1.66 μM and was titrated through the addition of small volumes (1–2 μl) of 5 mg/ml peptide stock solutions. UV absorbance spectra, acquired simultaneously with the CD measurements, are presented without correction in the supplementary materials to show the effects of light scattering and here, after being zeroed at 340 nm, to allow the absorbance at 260 nm to be followed more readily. The CD intensities at 272 nm were plotted as a function of the change in peptide to DNA molar ratios. The slope quoted for each peptide (Table 3) is the average of two independently repeated experiments.

2.4. Thiazole orange fluorescence intercalator displacement (FID)

Emission spectra of thiazole orange loaded onto the 15 base pair DNA duplex were acquired using a Cary Eclipse fluorimeter using an excitation wavelength of 519 nm and scanning from 520 nm to 600 nm. 1 ml of a 0.41 μM DNA solution loaded with thiazole orange in a 4 mm × 10 mm cuvette was titrated with small volumes of peptide. Normalized fluorescence intensity at 527 nm was plotted against the change in peptide/DNA molar ratio and fitted using the nonlinear curve fitting regime in Origin 8 (OriginLab Corporation, Northampton, MA) in order to extract an EC_{50}, defined as the peptide to DNA molar ratio that is required for half the available binding sites on the DNA to be occupied. The EC_{50} is used here as a qualitative comparison of the binding affinities of the peptides to the duplex DNA. While the binding response curves mostly displayed a strong sigmoidal character, the response of magainin 2 amide only could be described in terms of a single exponential. Binding characteristics extracted in this way are quoted (Table 3) as the average of two independent repeats of the assay.

2.5. Broth micro-dilution assay

The activities of the peptides against two strains of *E. coli* were assessed in planktonic suspension in polypropylene 96 well plates (Greiner Bio-one, Frickhausen, Germany) according to a modified broth dilution assay [11]. *E. coli* (NCTC 9001), competent *E. coli* TOP10 or *Pseudomonas aeruginosa* (PAO1) were grown without shaking in 50 ml Mueller-Hinton (MH) broth at 37 °C. Peptides were tested in duplicates with two rows allocated for each peptide. In each of columns 2–11, 50 μl of MH broth was added under sterile conditions. In the first row, 50 μl of 256 μg/ml stock peptide solutions prepared in distilled water were added and then the broth from the second row was pipette into the first row and thoroughly mixed before being deposited again in the second row. This process was repeated throughout the tray providing a twofold dilution of peptide with each row. Bacteria with an OD_{620} of 0.0001 were then added in volumes of 50 μl giving a further

Table 1
Comparison of physical and biological features of peptides used in this study. Hydrophobicity (*H*) and mean hydrophobic moment (μ*H*) are shown according to the Eisenberg scale [44] and were calculated using the HydroMCalc Java applet made available by Alex Tossi (http://www.bbcm.univ.trieste.it/~tossi/HydroCalc/HydroMCalc.html).
* Mean hydrophobic moment assuming formation of ideal α-helix.

Peptide	Sequence	Charge	(*H*)	(μ*H*)*
Buforin II amide	TRSSRAGLQFPVGRVHRLLRK-NH_2	+7	−0.37	0.3
Buforin F10W amide	TRSSRAGLQWPVGRVHRLLRK-NH_2	+7	−0.38	0.3
Buforin II	TRSSRAGLQFPVGRVHRLLRK	+6	−0.37	0.3
Magainin 2 amide	GIGKFLHSAKKFGKAFVGEIMNS-NH_2	+4	−0.03	0.28
Magainin F5W amide	GIGKWLHSAKKFGKAFVGEIMNS-NH_2	+4	−0.04	0.27
Pleurocidin amide	GWGSFFKKAAHVGKHVGKAALTHYL-NH_2	+5	−0.02	0.22
LAK	KKLAKALKLLALLWLKLAKALKKA-NH_2	+9	−0.09	0.34

twofold dilution and a final volume of 100 µl per well. The final column was used either as sterility control (100 µl broth) or negative control (no peptide). Plates were incubated overnight at 37 °C and the OD_{620} read. Growth curves prepared from duplicates were fitted to determine the peptide concentration required to inhibit growth by 50% (MIC_{50}). The MIC_{50} quoted for each peptide (Table 1) is an average value from four independent repeats.

3. Results

3.1. Circular dichroism—membrane binding

Circular dichroism (CD) measurements of the peptides in the presence of membrane mimetic media and lipid vesicles of differing composition provide information on the average secondary structure

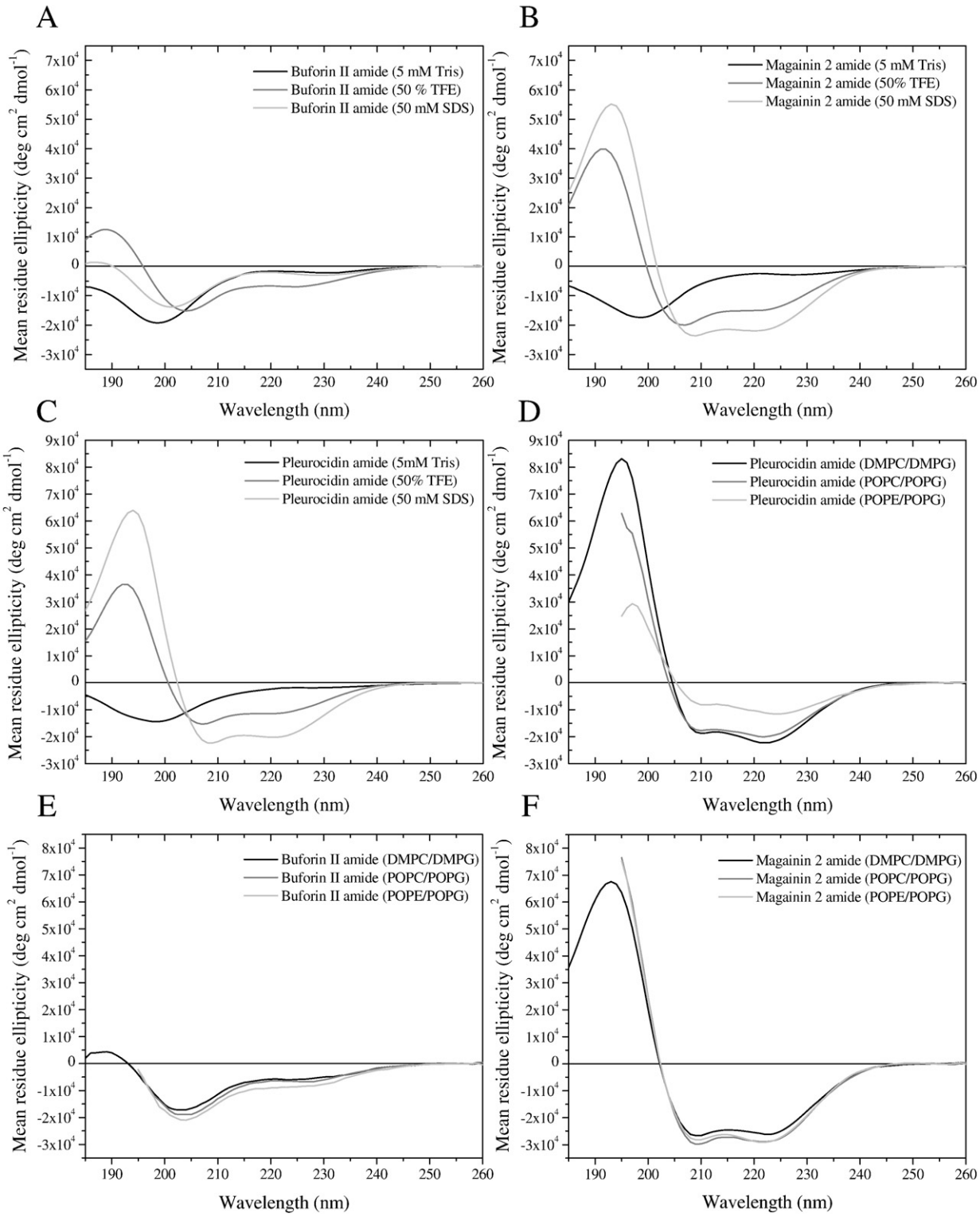

Fig. 1. Circular dichroism spectra of buforin II amide (A/E), magainin 2 amide (B/F) or pleurocidin amide (C/D) in solution (5 mM Tris pH 7, 50% TFE or 50 mM SDS) (A–C) or in the presence of various mixed anionic/zwitterionic lipid vesicles (D–F) where the anionic component comprised 20% of the lipid by mole and the peptide to lipid molar ratio was 1:200. The temperature was 37 °C and the final peptide concentration was 24 µM.

adopted by each peptide in each differing environment. Buforin II amide, magainin 2 amide and pleurocidin amide are all cationic peptides but each has a number of uncharged polar or hydrophobic residues. At lower concentrations, magainin 2 is known to adopt an amphipathic α-helical conformation in membranes with the helix long axis aligned parallel to the membrane surface [12–16]. This enables charged residues to interact with the polar or charged lipid headgroups while hydrophobic residues are oriented towards the hydrophobic core of the membrane. CD measurements of magainin 2 amide (Fig. 1B) and its tryptophan analogue (Supp. Fig. 1B) confirm that in aqueous solution both peptides adopt a disordered structure. As expected, in the presence of 50% TFE, which excludes water to promote intra-molecular hydrogen bonding, CD spectra are obtained that are consistent with a considerable ordered α-helical content. CD spectra indicating an even greater α-helical content are obtained in the presence of micelles formed by the anionic detergent SDS. Analyses of the spectra using CDPro provides a numerical estimate of the helical content (Table 2). Hence, in both membrane mimicking media, magainin 2 amide adopts a conformation with a substantial α-helical content. Pleurocidin amide behaves similarly to magainin 2 amide, both in aqueous solution and in membrane mimicking media (Fig. 1C). Buforin II amide has a greater overall charge and lower hydrophobicity than magainin 2 amide, but formation of an α-helix would lead to a separation of charged and hydrophobic residues giving a comparable hydrophobic moment (Table 1). The structure of buforin II has been determined previously using solution state NMR methodologies in 50% TFE [17]. The obtained conformation indicates a regular α-helix only between Val^{12} and Arg^{20} and, after the proline induced kink, a helical section with a pitch of −6.82 Å. This alternate helical arrangement ensures the amphipathic region extends from Arg^5 right through to Lys^{21} [17]. In the present study, the CD spectra of buforin II amide (Fig. 1A) and its tryptophan mutant (Supp. Fig. 1A) are indistinguishable from each other in aqueous or membrane mimicking environments (Table 2). CD indicates that both buforin II amide peptides adopt a disordered structure in aqueous solution. In 50% TFE, but not in the presence of SDS micelles, both buforin II amide peptides become more ordered. This behavior is distinctly different from both magainin 2 amide and pleurocidin amide. The sensitivity of the Chirascan spectrometer allows spectra with good signal-to-noise enabling measurements with peptide-to-lipid molar ratios as low as 1:200. At this ratio, sufficient negative charge is maintained, for liposomes with approximately 20 mol percent anionic lipid, after peptide binding that liposome aggregation and concomitant light scattering do not impair the measurements. Spectra obtained in this way are shown for a variety of liposome compositions (Fig. 1D–F); spectra obtained at the higher peptide-to-lipid molar ratio of 1:100 were similar (not shown) but at higher peptide-to-lipid molar ratios (circa 1:50), considerable light scattering was observed, compromising spectra particularly at shorter wavelengths. Three binary lipid mixtures were used with either DMPG or POPG as the anionic component and either POPC or POPE as the zwitterionic component. Membrane lipid charge ratios were chosen to match those of the inner membrane of *E. coli* with POPE/POPG (80:20) being the closest match. POPC/POPG or DMPG/DMPG allowed an assessment of the effect of changing the zwitterionic lipid headgroup or replacing mono-unsaturated acyl chains with saturated chains, respectively. At 37 °C, corresponding to physiological temperature for a bacterium within a human host, the CD spectra obtained for magainin 2 amide (Fig. 1F) and the F5W analogue (Supp. Fig. 1D) in these mixed lipid membranes and the CDPro analyses indicate that both peptides adopt an almost identical α-helix conformation to a much greater extent than in SDS micelles or 50% TFE. In this case, the SDS micelle is a better mimic for the liposome vesicle environment than 50% TFE. In contrast, buforin II amide (Fig. 1E) and the F10W analogue (Supp. Fig. 1C) show a greatly reduced tendency to becoming ordered in all the liposome environments; the very modest tendency to adopt any α-helical conformation correlates more with 50% TFE than SDS micelles. The α-helical content of buforin II, with a free C-terminus, was even lower than that of the amidated analogue in 50% TFE and all three lipid environments (Table 2). CD spectra obtained for pleurocidin amide in the same liposome environments (Fig. 1D) indicated that the peptide adopted an α-helix conformation, similar to that of the two magainin 2 amide peptides except when added to POPE/POPG membranes where a substantial reduction in α-helix conformation is observed when compared with magainin 2 amide in POPE/POPG and its own conformation in either POPC/POPG or DMPC/DMPG.

Table 2
Comparison of α-helix content derived from CDPro analysis of the spectra in Fig. 2. Spectra were analyzed between 260 and 185 nm in solution, 50% TFE and 50 mM SDS and between 260 and 195 nm for lipid suspensions.

Peptide	α-Helix content					
	5 mM Tris	50% TFE	50 mM SDS	DMPC/ DMPG	POPC/ POPG	POPE/ POPG
Buforin II amide	0.04	0.28	0.13	0.26	0.33	0.36
Buforin F10W amide	0.06	0.35	0.10	0.20	0.28	0.25
Buforin II amide	0.05	0.20	0.23	0.16	0.19	0.19
Magainin 2 amide	0.05	0.50	0.76	0.91	0.90	0.90
Magainin F5W amide	0.06	0.48	0.81	0.93	0.89	0.91
Pleurocidin amide	0.05	0.47	0.83	0.89	0.84	0.47

3.2. Thiazole orange fluorescence intercalating displacement assay

A thiazole orange fluorescent intercalating displacement (FID) assay [18] has been employed to determine the binding characteristics of the buforin and magainin peptides to a short DNA duplex. The reduction in fluorescence intensity from the DNA bound dye, following addition of increasing amounts of each peptide, is taken to be a measure of the fraction of peptide displacing the dye and binding to the DNA. The increase in the bound fraction of peptide is shown as a function of the peptide to DNA molar ratio (Fig. 2A). For all of the peptides, except magainin 2 amide, the decay of the fluorescence intensity has a clearly sigmoid form. Extracting values for the peptide/DNA molar ratio required for half of the dye to be displaced (EC_{50}) allows a comparison of the binding characteristics of each of the peptides (Table 3). Cationic AMPs are often amidated at the C-terminus to increase activity and in the present study we have studied amidated versions of buforin II and magainin 2, comparing like with like, but have also examined the binding of the non-amidated form of buforin II to assess the contribution of this modification. Buforin II amide and buforin F10W amide had the greatest affinity for the duplex DNA. The EC_{50} for these two peptides was nearly fourfold lower than that of magainin 2 amide, the difference also being significant ($p<0.05$). Buforin II, where the C-terminal is not amidated, had a binding affinity that was significantly greater than that of both magainin peptides ($p<0.05$) and not significantly weaker than that of the two amidated buforin peptides. Magainin 2 amide had the weakest binding affinity and was the only one of the peptides whose binding could be satisfactorily fitted with a single exponential. Mutation of Phe^5 to tryptophan caused an almost twofold increase in the affinity of magainin 2 to the duplex DNA which is also significant ($p<0.05$) and introduced a sigmoidal response to the binding and displacement mechanism. In contrast, the binding affinity of buforin II amide and buforin F10W amide were indistinguishable (Fig. 2B). Pleurocidin amide has intermediate DNA binding capabilities with an EC_{50} that was greater than that of the three buforin peptides but lower than those of the two magainin peptides.

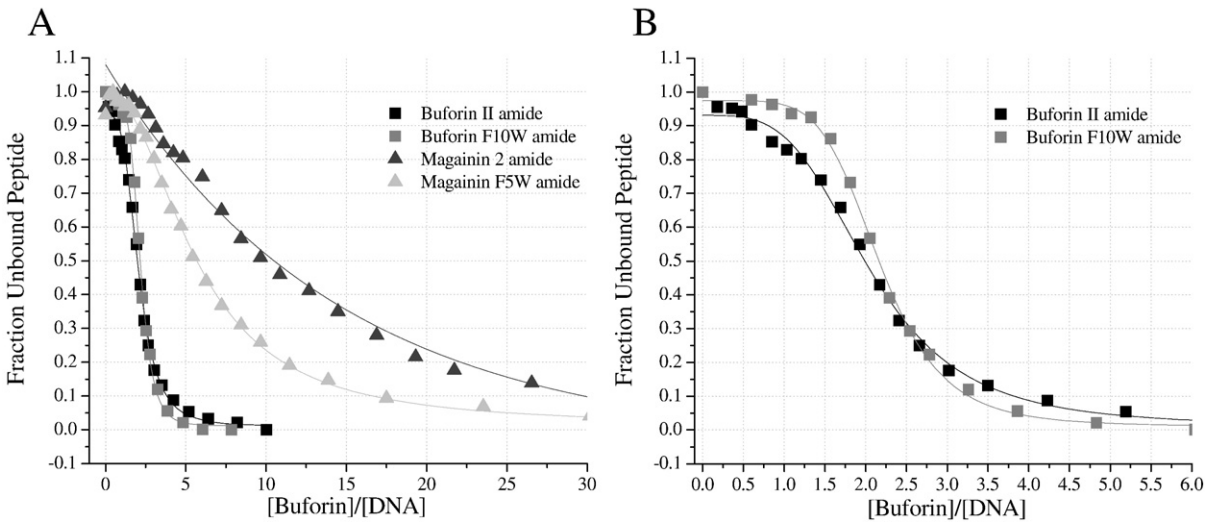

Fig. 2. Thiazole orange fluorescent indicator displacement assays performed at room temperature for buforin II amide, magainin 2 amide and their tryptophan containing mutants with the 15 base pair duplex DNA (A). The same data are shown on an expanded scale for buforin II amide and buforin F10W amide (B). The DNA concentration was 0.41 μM.

3.3. Circular dichroism—DNA binding

Near-UV circular dichroism spectra of the duplex DNA in solution are characteristic of those obtained for the B form of DNA (Fig. 3A, C, E). A strong positive signal is observed between 260 and 290 nm with, in this case, a shoulder observable around 272 nm. Similarly, a strong negative signal is observed between 230 and 260 nm. Near-UV spectra are suitable for monitoring the response of DNA to the addition of peptide. CD contributions above 250 nm due to peptide are negligible, despite the presence of phenylalanine and tryptophan residues in the peptide sequences (Supp. Fig. 4). Addition of small amounts of buforin II amide causes dramatic changes in both the CD spectra (Fig. 3A) and simultaneously obtained absorbance spectra (Fig. 3B). Initially the shoulder observed in the CD at 272 nm is seen to fall while the signal between 230 and 260 nm as well as the characteristic DNA absorbance at 260 nm remain unaffected. When between three and four molar equivalents of buforin II amide have been added to the complex, the absorbance at 260 nm begins to collapse with the onset of turbidity (Fig. 3B); circular intensity differential light scattering now dominates the CD spectrum as the DNA becomes condensed by the peptide. At this stage the CD spectra take on a greatly altered form as a positive intensity builds around 290 nm, the shoulder at 272 nm is completely absent and substantial rearrangements occur in the region between 230 and 260 nm. In contrast, the effects of magainin 2 amide on the same DNA duplex are much more moderate (Fig. 3C) with those of pleurocidin amide being intermediate between buforin II amide and magainin 2 amide (Fig. 3E). The CD shoulder at 272 nm, for DNA challenged with magainin 2 amide, is much more resistant to the addition of peptide and remains almost throughout the course of the experiment. The corresponding absorbance spectra show substantial hypochromism; the absence of turbidity (light scattering) above 310 nm indicates that the DNA remains in solution (Fig. 3D). The change in intensity of the CD (272 nm) is the most notable event in the initial stages of the peptide/DNA binding process and hence this is plotted as a function of peptide to DNA molar ratio (Fig. 4A) for as long as the DNA remains in solution. This allows the rate of change of this feature to be used as a means of providing a quantitative comparison of peptides with a putative DNA binding bactericidal strategy. A peptide concentration dependent reduction of the CD (272 nm) intensity is observed upon addition of peptide. Extracting a slope from these plots enables the structural rearrangements observed by CD to be related to the binding affinities and modes of the peptides (Table 3). This relationship between the binding affinity of the peptides and the structural changes is made more apparent by plotting the change in CD (272 nm) signal for each peptide as a function of the corresponding measured relative dissociation constant (Fig. 4B). This plot reveals the trend whereby the peptides with the greatest affinity for the DNA duplex also cause the greatest change in the CD (272 nm) signal. The two amidated buforin peptides have both the highest affinity for the DNA duplex and induce the greatest changes in CD, greater than those induced by either magainin peptide ($p<0.05$). Magainin 2 amide has the lowest affinity and induces the least change in CD. The observed increase in the effect of this peptide on the CD (272 nm) signal following replacement of Phe^5 with tryptophan however may or may not be significant ($p=0.165$). Equally, buforin II, with a free C-terminal, has both a slightly reduced affinity for the DNA duplex and also causes slightly less of an effect on the CD (272 nm) signal when compared with the amidated analogue which again may or may not be significant ($p=0.09$). Pleurocidin amide has intermediate binding affinity (Table 3) and is observed to also have an intermediate effect on the CD (272 nm) signal.

Finally, far-UV spectra were obtained to observe CD attributable to the peptide (Fig. 5A–D). In this region, the optical pathlength was 0.5 mm, twenty fold less than the 1 cm used in the near UV. Nucleic acid contributions are now less significant. In contrast with the structure

Table 3
Comparison of the DNA binding characteristics and antimicrobial activities of the cationic peptides. Dissociation constant (EC_{50}) derived from thiazole orange FID assay.

Peptide	EC_{50}	ΔCD @ 272 nm	MIC_{50}		
			E. coli (NCTC 9001)	*E. coli* (TOP10)	*P. aeruginosa* (PAO1)
Buforin II amide	2.51 ± 0.64	−0.198 ± 0.007	>26.30	>26.30	>26.30
Buforin F10W amide	2.52 ± 0.49	−0.220 ± 0.016	>25.89	>25.89	>25.89
Buforin II	3.78 ± 0.29	−0.133 ± 0.029	>26.28	>26.28	>26.28
Magainin 2 amide	9.45 ± 0.71	−0.066 ± 0.024	6.86 ± 1.58	1.79 ± 0.13	10.60 ± 2.21
Magainin F5W amide	5.29 ± 0.50	−0.113 ± 0.020	4.21 ± 1.29	1.25 ± 0.28	7.29 ± 2.73
Pleurocidin amide	4.32 ± 0.80	−0.121 ± 0.003	0.66 ± 0.22	0.18 ± 0.02	1.65 ± 0.87

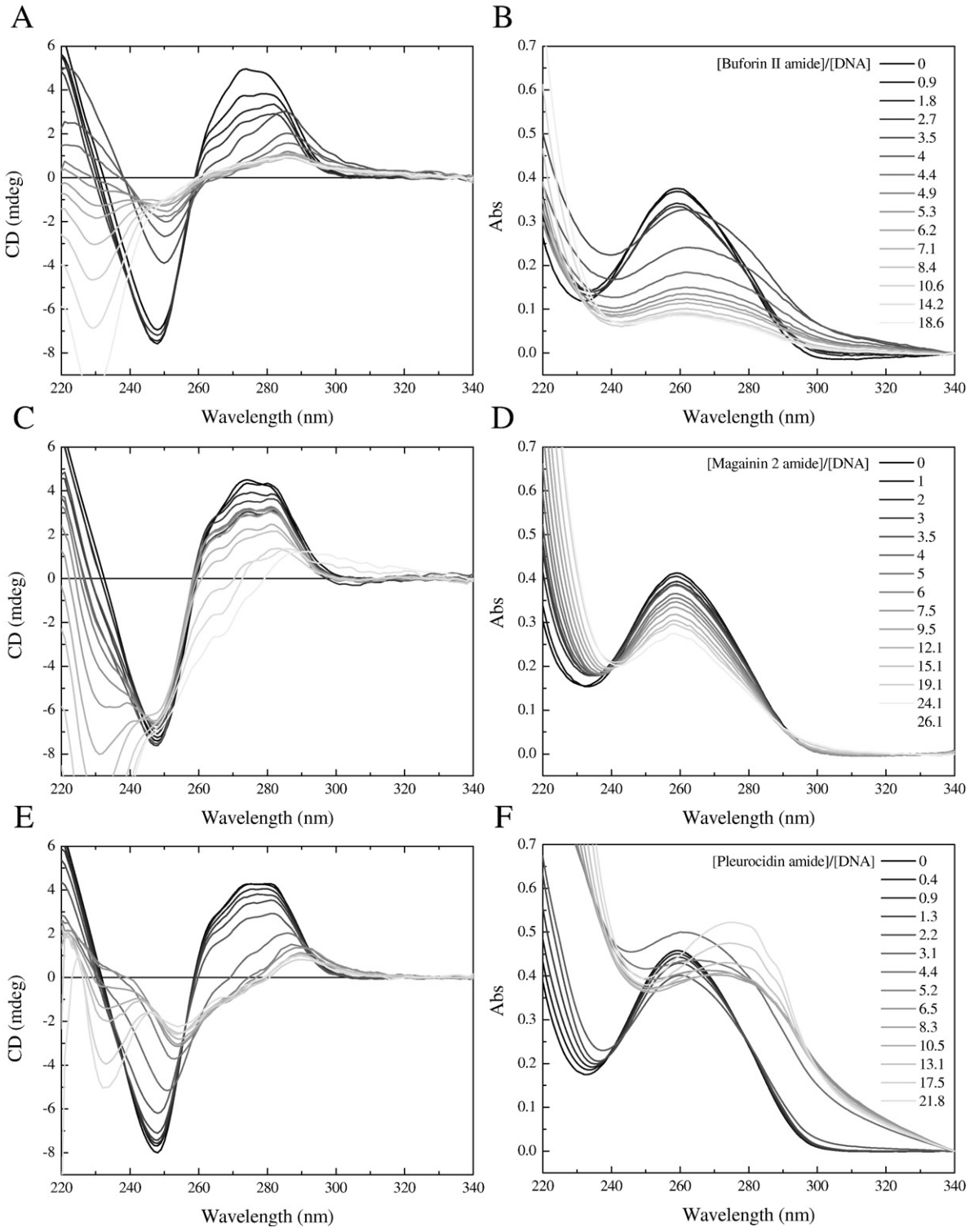

Fig. 3. Typical circular dichroism (A, C) and zeroed UV (B, D) spectra of 15 base pair duplex DNA incubated with increasing amounts of either buforin II amide (A, B) or magainin 2 amide (C, D) at room temperature. The DNA concentration was typically between 1 and 2 μM. The peptide to DNA molar ratios are given.

determined by NMR and with the far-UV spectra described above for buforin II in membrane or membrane mimicking environments, little or no evidence of an α-helical conformation is observed for buforin II amide bound to duplex DNA (Fig. 5A). Instead, in the spectra acquired at [peptide]/[DNA] ratios below 4, the strong negative CD signal at around 195 nm coupled with the absence of a negative band between 220 and 230 nm suggests the peptide adopts an extended conformation. Further work is required to distinguish between a disordered or polyproline II conformation. At peptide to DNA molar ratios below 4, the negative band has a negative maximum at 195 nm which shifts toward 199 nm as more peptide is added (Fig. 5A). These spectra, recorded at peptide to DNA molar ratios greater than 4, have greater contributions from peptides either in solution or not directly bound to DNA. Notably, a negative maximum of 199 nm is observed for buforin II amide in solution (Fig. 1A). This suggests a possible polyproline II conformation [19] for those peptide molecules directly bound to the DNA duplex.

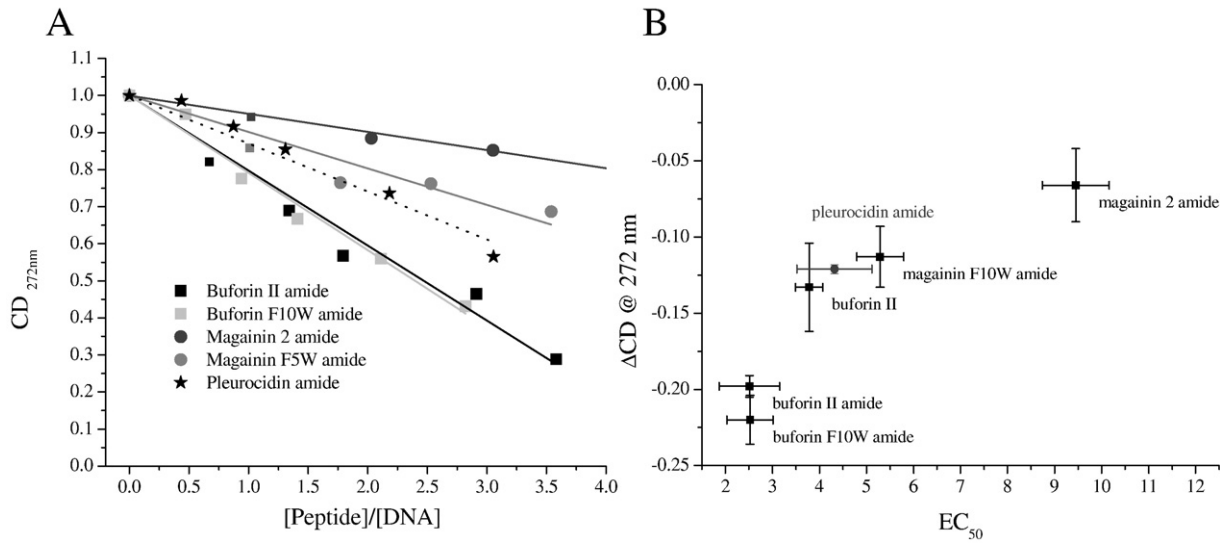

Fig. 4. The change in normalized CD as a function of peptide to duplex DNA molar ratio reveals the differential effect of five peptides on molecular CD events (A). The change in normalized CD at 272 nm (as shown in panel A) is plotted as a function of the relative dissociation constant (EC_{50}) for each peptide revealing the relationship between the two parameters (B).

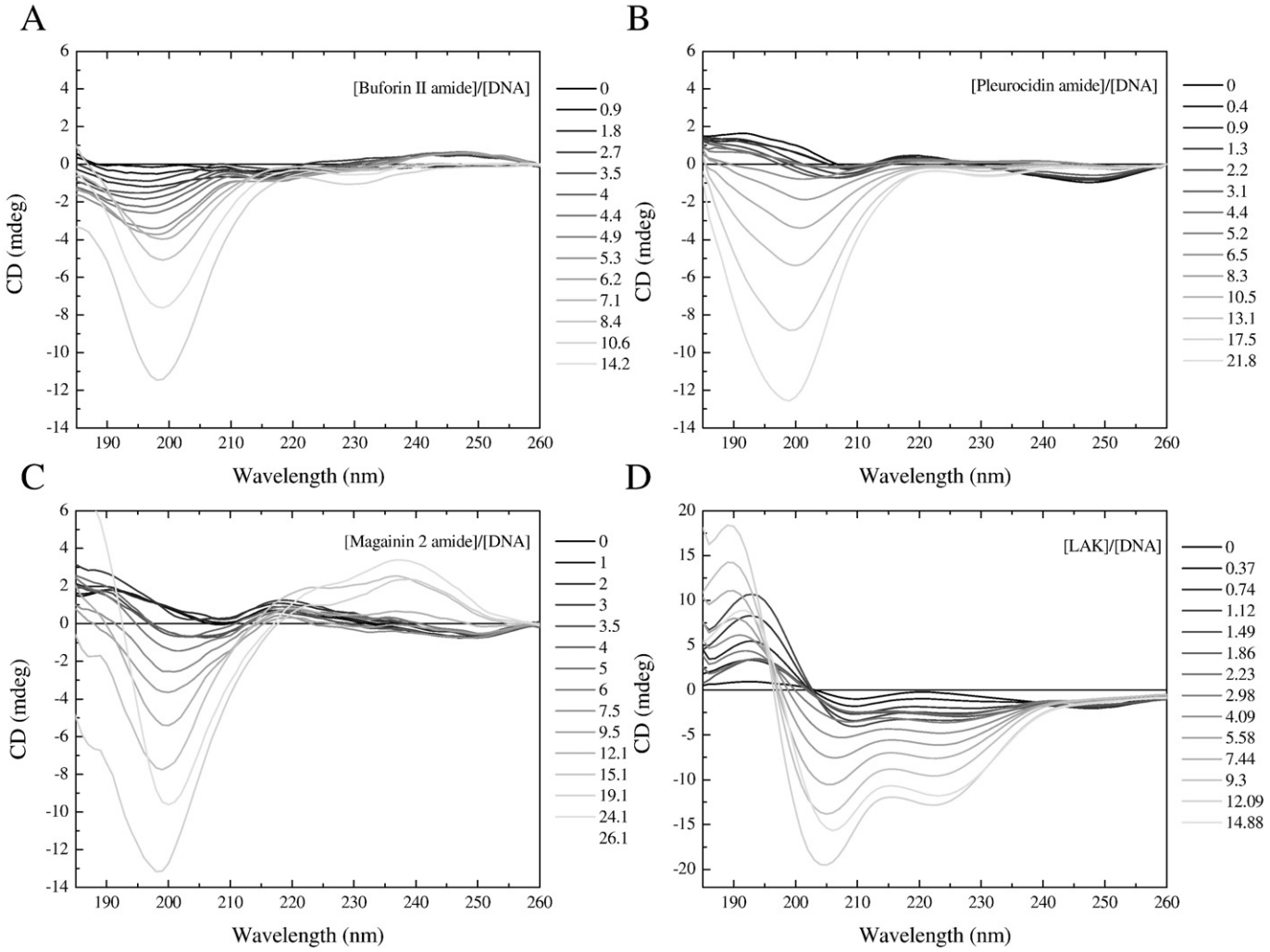

Fig. 5. Comparison of far-UV circular dichroism spectra for buforin II amide (A), pleurocidin amide (B), magainin 2 amide (C) and LAK (D) reveals the conformation of the peptide bound to the DNA duplex. Spectra obtained at peptide to DNA molar ratios between 0 and 4, with darker traces, likely correspond to peptide directly bound to DNA. Lighter traces, for spectra at higher peptide to DNA molar ratios, will have contributions from non-annular bound peptides or peptides remaining in solution.

However, unequivocal attribution of such a conformation is difficult without observation of an expected, weak, positive band around 215 nm which would be obscured in the present experiment by signals from the DNA duplex. Nevertheless, the experimental evidence strongly indicates that buforin II amide does not bind to duplex DNA in an α-helix conformation. Similar experiments were performed for pleurocidin amide (Fig. 5B) and magainin 2 amide (Fig. 5C). Again focusing on spectra recorded at peptide:DNA ratios <4, no evidence of an α-helix conformation is observed. For comparison, a similar experiment was performed with a designed cationic peptide, LAK (Fig. 5D), which has a comparable effect to that of buforin II amide, on the near-UV spectra of the duplex DNA (Supp. Fig. 3). At peptide-to-DNA ratios below 4, this peptide adopts an α-helical structure when bound in a peptide-DNA complex, according to the strong negative bands at 205 and 220 nm and strong positive band at 195 nm observed in the corresponding far-UV spectra (Fig. 5D). The LAK peptide is designed to adopt an almost perfect amphipathic α-helix in media that support such conformations and is used here to highlight the ability of the far-UV CD spectra to identify an α-helix conformation in peptides bound to the DNA duplex. In contrast, such α-helix conformation is clearly absent from buforin II amide, magainin 2 amide or pleurocidin amide when bound to DNA.

3.4. Broth micro-dilution assay

The antibiotic activity of the peptides was tested against two separate strains of *E. coli* and one of *P. aeruginosa*. NCTC 9001 is a type strain while TOP10 is a competent strain with a genotype similar to that of DH10B which is deficient in *galU*, *galK* and *galE* [20]. Inactivation of *galE* perturbs the incorporation of glucose into the O-side chain of lipopolysaccharide (LPS) and hence *E. coli* TOP10 are expected to have an altered LPS structure. *E. coli* TOP10 were more susceptible to AMP challenge than the type strain while the amidated magainin peptides were substantially more effective than the corresponding amidated buforin peptides against both strains (Table 3). The buforin peptides had only a modest affect on bacterial growth at the highest peptide concentration tested, insufficient for the determination of an MIC, and no differences in activity were observed between buforin II with either free or amidated C-termini or between buforin II amide and buforin F10W amide. Buforin peptides have previously been reported to have anti-bacterial activities that far surpass those of magainin 2 [21]. The previous report used an agar diffusion protocol where the bacterial cells were washed in cold 10 mM sodium phosphate buffer prior to challenge. Our procedure involves challenge of planktonic cultures of bacteria, according to commonly used procedures [11], and is consistent with the observation that phosphatidylethanolamine lipids, abundant in the membranes of Gram-negative organisms, abolish the membrane translocation of buforin II necessary for its supposed intracellular targeting antibacterial strategy [22]. Interestingly, a small but significant enhancement of activity was observed for magainin F5W amide over magainin 2 amide against both strains of *E. coli* ($p<0.05$) and may apply also against *P. aeruginosa* ($p=0.07$).

4. Discussion

Cationic AMPs are diverse in structure and mechanisms of action [5,6] and therefore present an interesting challenge to those using a rational design strategy to develop them as anti-infective therapeutic compounds [1–4]. While it is recognized that AMPs with unrelated structural properties may operate with distinct mechanisms [5,6] it has also been suggested that it is sufficient for a peptide to satisfy a set of physico-chemical conditions for broad spectrum antibacterial activity to be conferred [23]. The argument follows that secondary structure is unimportant for the activity of AMPs and that directed combinatorial methods will be the most fruitful path to incremental increases in the potency of AMPs. However, data from the same study indicates that disrupting secondary structure in AMPs dramatically reduces activity against Gram negative bacteria [23], indicating that secondary structure is important for activity against organisms such as *E. coli* and *P. aeruginosa* but not Gram positive bacteria. The composition of bacterial membranes varies considerably from species to species and has been shown to be an important predictor of antimicrobial potency [24]. Furthermore, biophysical evidence is emerging that shows that the pore forming behavior of an individual peptide will vary considerably according to the membrane composition [25,26]. Taken together, these reports suggest that understanding the structural contributions to species specific mechanisms of action will enable the design of peptides that can target bacteria with defined characteristics.

Pexiganan, or MSI-78, is a highly potent AMP derived from magainin 2, a naturally occurring peptide identified in the skin of the African frog *Xenopus laevis*. Pexiganan is the best studied AMP for therapeutic purposes to date and it, like magainin 2, is an amphipathic α-helical peptide proposed to operate via the formation of toroidal pores in bacterial membranes [27,28]. Measurements employing a variety of biophysical methods indicate that magainin 2 binds to membranes in an orientation with the long axis of the helix parallel to the membrane surface [13–16] but then, as its concentration in the membrane increases above a certain threshold, neutron in-plane scattering studies suggest a trans-membrane alignment is adopted which enables the peptides to line a toroidal shaped pore [28,29]. Interestingly however, both molecular dynamics simulations and experimental studies have shown that related cationic amphipathic α-helical peptides, including magainin H2 and pleurocidin amide, are capable of forming pores at concentrations where a surface alignment for the peptide is maintained [30–32]. The molecular dynamics study further revealed that, under these conditions, magainin H2 was capable of translocating from the external to the internal leaflet of the membrane [30], as has been observed experimentally for magainin 2 [24]. Furthermore, the potent antibacterial activity of designed amphipathic α-helical peptides has been shown, in a recent study [33], to be unrelated to their ability to form pores. Suspecting an intracellular targeting strategy for these peptides, we are interested in understanding the structural properties that underpin this alternative mechanism of antibacterial action.

Buforin II is a potent AMP which has been shown to kill bacteria by penetrating the cell membrane and inhibiting cellular functions [7,34]. Buforin II translocates across model membranes causing minimal disruption to the membrane [35] but, as the translocation of both buforin II and magainin 2 are inhibited by negative-curvature inducing lipids including phosphatidylethanolamine (PE), there have been proposed to be both similarities [22] and strong differences [35] between the translocation mechanisms of these peptides. The role of Pro^{11} in the translocation of buforin II is crucial as mutation of this residue abrogates the ability of the peptide both to translocate across model membranes without disrupting the membrane and penetrate *E. coli* cells [35,36]. In the NMR structure, determined in a mixture of H_2O and TFE, the Pro^{11} residue distorts the helix affecting the positioning of hydrophobic and charged residues [17]. Previous CD measurements indicate that this structure is maintained in anionic lipid membranes [35] while the present study confirms this structure is also maintained in mixed anionic/zwitterionic membranes designed to mimic those of Gram negative bacteria. This result contradicts a recently reported combined molecular dynamics (MD) and CD based analysis [37]. The MD study showed an increased proportion of α-helix in the N-terminal region of buforin II in the presence of PE lipids and interpreted CD with mixed POPE/POPG vesicles as having a greater α-helical character. However, the molecular dynamics study did not adequately reproduce existing experimental data. In the MD simulations, the α-helical conformation of the peptide was maintained in an aqueous environment while the peptide also bound to neutral lipid membranes. Both these results

contradict experimental results showing buforin II adopts a disordered structure in aqueous solution and does not bind to vesicles comprising zwitterionic lipids only [35]. The CD spectra obtained in support of these simulations were obtained at 25 °C, the phase transition temperature of POPE, and at peptide-to-lipid ratios where we have seen considerable impairment of the spectra from light scattering due to charge neutralization of the anionic liposomes by cationic peptide. Such light scattering is evident in the reported spectra [35]. According to its supposed mode of action, buforin II is proposed to readily translocate across bacterial membranes. Lipids, such as egg yolk L-α-phosphatidylethanolamine (EYPE), which induce negative membrane curvature, abolish such translocation however [34]. The membrane order in the POPE/POPG and DMPC/DMPG systems will be considerably greater than that of the POPC/POPG [38,39], as a result of the small ethanolamine headgroup size and saturated chains respectively. These differing membrane environments might be expected to exert considerable influence on the secondary structure of membrane inserted peptides. However, since the present study indicates both buforin II and buforin II amide adopt a very similar conformation in each of the three mixed zwitterionic/anionic membranes and that the nature of the zwitterionic lipid has little or no effect on the structure adopted by the peptide, a conformational change in buforin II is therefore not implicated in the mechanism by which PE lipids inhibit its translocation. In model membranes, the α-helical content of buforin II with a free C-terminus was lower still than the two amidated analogues, supporting a role for C-terminal amidation in aiding membrane insertion, as observed for other cationic α-helical AMPs [40].

Mutations in the buforin sequence have been shown experimentally to reduce binding of peptide to a DNA duplex and impair the antibacterial activity of the peptide [9]. Seeking to understand the structural properties of buforin that underpin its ability to bind DNA, we devised a combined FID and CD approach to monitor the binding and structural responses of both peptides and DNA when a series of antibacterial peptides bind to a DNA duplex, identical in sequence to that in the previous study [9]. Both the FID assay and CD study of peptide binding to duplex DNA in the present work confirm previous reports that buforin II has a high affinity for nucleic acids [7]. Interestingly, we have shown that the binding affinity of each peptide is reflected in the conformational changes observed in the corresponding near-UV CD spectra. The method is also sufficiently sensitive to detect that mutation of Phe^5 to tryptophan in magainin 2 amide increased the binding affinity for DNA and affected the apparent mode of binding which may be related to a modest enhancement in the antibacterial activity. The sigmoidal response of the FID assay might be taken to suggest cooperativity in the mode binding of the peptides to duplex DNA, with the exception of magainin 2 amide. However, this may not accurately reflect the situation within bacteria nor, indeed, in the near-UV CD experiments. The binding parameters obtained from the FID assay are influenced not only by the binding of peptide to DNA but by the competitive binding of the dye. With two competing binding processes, the data from the FID assay may either exaggerate cooperativity or suggest cooperativity that would otherwise not be present were it not for the presence of dye and hence, at present, we restrict our analysis to a qualitative comparison of the dissociation constants determined for each peptide.

Binding of buforin II amide to duplex DNA induced strong changes in the CD spectra attributable to the DNA duplex. The origin of the observed changes in the CD spectra is presently unknown but may occur as a result of changes in base-pair stacking and/or geometry of the double helix as CD spectra of nucleic acids are known to be sensitive to these parameters [41]. Hypochromism observed in the DNA UV absorption at 260 nm is strong evidence that the duplex conformation remains with stronger base-base interactions. For each of the peptides included in the present study, the UV/CD spectra associated with the peptide/DNA titration indicating a two-step process needs to be considered. The first step, up to peptide-to-DNA mole ratios of 3.5, involves simply the binding of the peptide; above a mole ratio greater than 3.5, charge neutralization with the formation of peptide–DNA–ψ-condensates dominates. Concentration dependent changes in molecular CD, with no sigmoidal character, were observable as up to four molar equivalents of peptide were added to the DNA duplex. This amount of peptide was sufficient to displace more than 90% of the dye in the corresponding FID assay. Adding more than four molar equivalents of buforin II amide to the DNA duplex leads to the formation of a DNA condensate with the spectra then dominated by circular intensity differential light scattering. The spectra obtained for buforin II amide DNA condensates are similar in appearance to those observed for positive ψ condensates formed by incubating DNA with poly(lysine-alanine) and are indicative of the formation of structures with long range order [42]. Interestingly buforin II amide, bound to the DNA duplex in the concentration range inducing the initial changes in near-UV CD, is shown to adopt an extended conformation rather than the helical conformation adopted in membranes or proposed from an MD simulation study [9]. Again the experimental data does not support the existing view provided by simulations and further work is required to develop a combined experimental/simulation approach in order to understand how the extended buforin II peptides condense duplex DNA.

The ability of a third antibacterial peptide, pleurocidin amide, to complex and condense DNA was also assessed. Pleurocidin amide had a reduced ability to bind DNA when compared with buforin II amide but had stronger interactions with the duplex than either of the two magainin peptides. Of the peptides tested in the present study, pleurocidin amide had by far the greatest activity against the Gram-negative organisms *E. coli* and *P. aeruginosa*. However, as pleurocidin amide demonstrated only intermediate DNA binding activity, this property cannot completely account for the high antibacterial potency of the peptide. Nevertheless, the DNA binding properties of pleurocidin amide may make some contribution to its potency and are consistent with previous reports of pleurocidin and its derivatives, including pleurocidin amide, entering *E. coli* and inhibiting macromolecular synthesis [43]. As noted above, pleurocidin amide interacts with mixed zwitterionic/anionic membranes in a similar fashion to magainin peptides, adopting a surface alignment and specifically disordering the acyl chains of anionic lipids in such membranes [30]. In the present study, Chirascan CD measurements have allowed a more sophisticated investigation of the conformations adopted by pleurocidin amide. Interestingly, though pleurocidin amide adopts a very similar α-helix conformation to magainin 2 amide in solution and most membrane mimicking environments, in phosphatidylethanolamine rich membranes a conformation with a lower content of α-helix is preferred. The link between this membrane conformation, observed for pleurocidin amide in membranes mimicking those of Gram-negative bacteria, and its translocation abilities would throw light on the mechanism underpinning the translocation of antimicrobial peptides into their bacterial targets.

5. Conclusion

The present study demonstrates that the conformation adopted by buforin II amide when binding to, and condensing, duplex DNA differs from that adopted in membranes. The conformation of buforin II amide in membranes is not dominantly α-helix and the peptide has poor membrane translocation ability compared with magainin 2 amide, which is strongly α-helical and capable of translocating membranes composed of lipids found in the membranes of Gram-negative bacteria. Since α-helix conformation appears important for membrane translocation but not for DNA binding and condensation, potent antibacterial peptides can be considered in the future that are

capable of adopting structures that promote membrane translocation, DNA binding and DNA condensation.

Acknowledgments

This work was supported by the Medical Research Council (NIRG to AJM), the Wellcome Trust (VIP Award to AJM and Capital Award for the KCL Centre for Biomolecular Spectroscopy), the University of London Central Research Fund (AR/CRF/B) and Applied Photophysics. We are grateful to Drs K.D. Bruce and T. Spasenovski for their assistance in setting up antibacterial testing in the Molecular Microbiology Research Laboratory (PSD).

Appendix A. Supplementary data

Supplementary data associated with this article can be found, in the online version, at doi:10.1016/j.bbamem.2010.07.003.

References

[1] R.E.W. Hancock, H.-G. Sahl, Antimicrobial and host-defense peptides as new anti-infective therapeutic strategies, Nat. Biotechnol. 24 (2006) 1551–1557.
[2] K.V.R. Reddy, R.D. Yedery, C. Aranha, Antimicrobial peptides: premises and promises, Int. J. Antimicrob. Agents 24 (2004) 536–547.
[3] A.K. Marr, W.J. Gooderham, R.E.W. Hancock, Antibacterial peptides for therapeutic use: obstacles and realistic outlook, Curr. Opin. Pharmacol. 6 (2006) 468–472.
[4] Y.J. Gordon, E.G. Romanowski, A.M. McDermott, A review of antimicrobial peptides and their therapeutic potential as anti-infective drugs, Curr. Eye Res. 30 (2005) 505–515.
[5] K.A. Brogden, Antimicrobial peptides: pore formers or metabolic inhibitors in bacteria? Nat. Rev. Microbiol. 3 (2005) 238–250.
[6] J.D.F. Hale, R.E.W. Hancock, Alternative mechanisms of action of cationic antimicrobial peptides on bacteria, Expert Rev. Anti Infect. Ther. 5 (2007) 951–959.
[7] C.B. Park, H.S. Kim, S.C. Kim, Mechanism of action of the antimicrobial peptide buforin II: Buforin II kills microorganisms by penetrating the cell membrane and inhibiting cellular functions, Biochem. Biophys. Res. Commun. 244 (1998) 253–257.
[8] O. Cirioni, et al., Therapeutic efficacy of buforin II and rifampin in a rat model of *Acinetobacter baumanii* sepsis, Crit. Care Med. 37 (2009) 1403–1407.
[9] E.T. Uyterhoeven, C.H. Butler, D. Ko, D.E. Elmore, Investigating the nucleic acid interactions and antimicrobial mechanism of buforin II, FEBS Lett. 582 (2008) 1715–1718.
[10] N. Sreerama, R.W. Woody, Estimation of protein secondary structure from CD spectra: comparison of CONTIN, SELCON and CDSSTR methods with an expanded reference set, Anal. Biochem. 287 (2000) 252–260.
[11] I. Wiegand, K. Hilpert, R.E.W. Hancock, Agar and broth dilution methods to determine the minimal inhibitory concentration (MIC) of antimicrobial substances, Nat. Protoc. 3 (2008) 163–175.
[12] B. Bechinger, M. Zasloff, S.J. Opella, Structure and interactions of magainin antibiotic peptides in lipid bilayers: a solid-state nuclear magnetic resonance investigation, Biophys. J. 62 (1992) 12–14.
[13] B. Bechinger, M. Zasloff, S.J. Opella, Structure and orientation of the antibiotic peptide magainin in membranes by solid-state nuclear magnetic resonance spectroscopy, Protein Sci. 2 (1993) 2077–2084.
[14] B. Bechinger, J.M. Ruysschaert, E. Goormaghtigh, Membrane helix orientation from linear dichroism of infrared attenuated total reflection spectra, Biophys. J. 76 (1999) 552–563.
[15] K. Matsuzaki, O. Murase, H. Tokuda, S. Funakoshi, N. Fujii, K. Miyajima, Orientational and aggregational states of magainin 2 in phospholipid bilayers, Biochemistry 33 (1994) 3342–3349.
[16] S.J. Ludtke, K. He, Y. Wu, H.W. Huang, Cooperative membrane insertion of magainin correlated with its cytolytic activity, Biochim. Biophys. Acta 1190 (1994) 181–184.
[17] G.-S. Yi, C.B. Park, S.C. Kim, C. Cheong, Solution structure of an antimicrobial peptide buforin II, FEBS Lett. 398 (1996) 87–90.
[18] D.L. Boger, W.C. Tse, Thiazole Orange as the fluorescent intercalator in a high resolution FID assay for determining DNA binding affinity and sequence selectivity of small molecules, Bioorg. Med. Chem. 9 (2001) 2511–2518.
[19] R.W. Woody, Circular dichroism spectrum of peptides in poly(pro)II conformation, J. Am. Chem. Soc. 131 (2009) 8234–8245.
[20] T. Durfee, et al., The complete genome sequence of *Escherichia coli* DH10B: insights into the biology of a laboratory workhorse, J. Bacteriol. 190 (2008) 2597–2606.
[21] C.B. Park, M.S. Kim, S.C. Kim, A novel antimicrobial peptide from *Bufo bufo gargarizans*, Biochem. Biophys. Res. Commun. 218 (1996) 408–413.
[22] S. Kobayashi, A. Chikushi, S. Tougu, Y. Imura, M. Nishida, Y. Yano, K. Matsuzaki, Membrane translocation mechanism of the antimicrobial peptide buforin 2, Biochemistry 43 (2004) 15610–15616.
[23] R. Rathinakumar, W.F. Walkenhorst, W.C. Wimley, Broad-spectrum antimicrobial peptides by rational combinatorial design and high-throughput screening: the importance of interfacial activity, J. Am. Chem. Soc. 131 (2009) 7609–7617.
[24] R.M. Epand, S. Rotem, A. Mor, B. Berno, R.F. Epand, Bacterial membranes as predictors of antimicrobial potency, J. Am. Chem. Soc. 130 (2008) 14346–14352.
[25] S.M. Gregory, A. Pokorny, P.F.F. Almeida, Magainin 2 revisited: a test of the Quantitative Model for the all-or-none permeabilization of phospholipid vesicles, Biophys. J. 96 (2009) 116–131.
[26] P.F.F. Almeida, A. Pokorny, Mechanisms of antimicrobial, cytolytic, and cell-penetrating peptides: from kinetics to thermodynamics, Biochemistry 48 (2009) 8083–8093.
[27] L.M. Gottler, A. Ramamoorthy, Structure, membrane orientation, mechanism, and function of pexiganan—a highly potent antimicrobial peptide designed from magainin, Biochim. Biophys. Acta 1788 (2009) 1680–1686.
[28] S.J. Ludtke, K. He, W.T. Heller, T.A. Harroun, L. Yang, H.W. Huang, Membrane pores induced by magainin, Biochemistry 35 (1996) 13723–13728.
[29] H.W. Huang, Molecular mechanism of antimicrobial peptides: the origin of cooperativity, Biochim. Biophys. Acta 1758 (2006) 1292–1302.
[30] H. Leontiadou, A.E. Mark, S.J. Marrink, Antimicrobial peptides in action, J. Am. Chem. Soc. 128 (2006) 12156–12161.
[31] A.J. Mason, I.N.H. Chotimah, P. Bertani, B. Bechinger, A spectroscopic study of the membrane interaction of the antimicrobial peptide Pleurocidin, Mol. Membr. Biol. 23 (2006) 185–194.
[32] N. Saint, H. Cadiou, Y. Bessin, G. Molle, Antibacterial peptide pleurocidin forms ion channels in planar lipid bilayers, Biochim. Biophys. Acta 1564 (2002) 359–364.
[33] A.J. Mason, et al., Structural determinants of antimicrobial and antiplasmodial activity and selectivity in histidine-rich amphipathic cationic peptides, J. Biol. Chem. 284 (2009) 119–133.
[34] J.H. Cho, B.H. Sung, S.C. Kim, Buforins: histone H2A-derived antimicrobial peptides from toad stomach, Biochim. Biophys. Acta 1788 (2009) 1564–1569.
[35] S. Kobayashi, K. Takeshima, C.B. Park, S.C. Kim, K. Matsuzaki, Interactions of the novel antimicrobial peptide Buforin 2 with lipid bilayers: proline as a translocation promoting factor, Biochemistry 39 (2000) (2000) 8648–8654.
[36] C.B. Park, K.-S. Yi, K. Matsuzaki, M.S. Kim, S.C. Kim, Structure-activity analysis of buforin II, a histone H2A-derived antimicrobial peptide: the proline hinge is responsible for the cell penetrating ability of buforin II, Proc. Natl. Acad. Sci. U. S. A. 97 (2000) 8245–8250.
[37] E. Fleming, N.P. Maharaj, J.L. Chen, R.B. Nelson, D.E. Elmore, Effect of lipid composition on buforin II structure and membrane entry, Proteins 73 (2008) 480–491.
[38] A.J. Mason, A. Marquette, B. Bechinger, Zwitterionic phospholipids and sterols modulate antimicrobial peptide-induced membrane destabilization, Biophys. J. 93 (2007) 4289–4299.
[39] J. Tuchtenhagen, W. Ziegler, A. Blume, Acyl chain conformational ordering in liquid-crystalline bilayers: comparative FT-IR and ^{2}H-NMR studies of phospholipids differing in headgroup structure and chain length, Eur. Biophys. J. 23 (1994) 323–335.
[40] Y.-L. Pan, J.T.-J. Cheng, J. Hale, J. Pan, R.E.W. Hancock, S.K. Straus, Characterization of the structure and membrane interaction of the antimicrobial peptides Aurein 2.2 and 2.3 from Australian southern bell frogs, Biophys. J. 92 (2007) 2854–2864.
[41] I. Tinoco Jr, C. Bustamente, M.F. Maestre, The optical activity of nucleic acids and their aggregates, Annu. Rev. Biophys. Bioeng. 9 (1980) 107–141.
[42] C.L. Phillips, W.E. Mickols, M.F. Maestre, I. Tinoco Jr., Circular differential scattering and circular differential absorption of DNA–protein condensates and of dyes bound to DNA–protein condensates, Biochemistry 25 (1986) 7803–7811.
[43] A. Patrzykat, C.L. Friedrich, L. Zhang, V. Mendoza, R.E.W. Hancock, Sublethal concentrations of Pleurocidin-derived antimicrobial peptides inhibit macromolecular synthesis in *Escherichia coli*, Antimicrob. Agents Chemother. 46 (2002) 605–614.
[44] D. Eisenberg, R.M. Weiss, C.T. Terwilliger, W. Wilcox, Hydrophobic moments and protein structure, Faraday Symp. Chem. Soc. 17 (1982) 109–120.